International Journal of Heat and Mass Transfer 52 (2009) 1980–1990

Contents lists available at ScienceDirect

International Journal of Heat and Mass Transfer

journal homepage: www.elsevier.com/locate/ijhmt

Variations in gas properties in laminar micro-convection with entrance effect

Nitin P. Gulhane, Shripad P. Mahulikar *

Department of Aerospace Engineering, Indian Institute of Technology Bombay, P.O. IIT Powai, Mumbai 400076, India

ARTICLE INFO

Article history:
Received 2 January 2008
Received in revised form 22 June 2008
Available online 16 December 2008

Keywords:
Entrance effect
Graetz problem
Micro-flow
Nusselt number

ABSTRACT

The present work investigates the influence of property variations of air in laminar forced convection with entrance effect. Two-dimensional micro-sized geometry (with axisymmetry) with constant wall heat flux boundary condition is considered to predict flow behaviour and thermal development. The continnum-based conservation equations are numerically solved to account for non-rarefaction scaling effects due to variations in fluid properties. At the microscale, results for Nusselt number show significant deviation from conventional theory that does not consider additional mechanisms that surface. The effect of property variation in Graetz problem for low subsonic flow is also studied.

1. Introduction

High heat flux dissipation technique [1] using liquid/gas as coolant is suitable for compact microscale devices. Over last few years, industries are focusing on miniaturized, high-performance and high-speed electronic devices like MEMS, MST, μ-TAS. These devices are having advanced applications in diverse areas viz. micro-electronic, aviation, metrology, micro-robot, micro-satellite, micro-engine and bioengineering. Micro-convection has been identified as research area in transport phenomena, therefore, understanding its characteristics is important. In past several researchers [2–5] have experimentally and theoretically investigated heat transfer characteristics at microscale. Their experimental investigation indicates that conventional correlations are no longer applicable. The results are deviated due to geometric configuration, fluid properties, surface roughness and viscous dissipation. To explain these departures from known characteristics, modification to the boundary conditions is given by scaling effect [6]. The most updated state-of-the-art review of single phase micro-convection has been illustrated by Morini [7]. Steinke and Kandlikar [8] have extensively reviewed literature on experimental investigation of microscale fluid flow and found diversity in experimental results from conventional theory. Sobhan and Garimella [9] prepared a comparative analysis to focus on anomalies and deviations from the behaviour expected for conventional channels. In comprehensive review, Mahulikar et al. [10] reported that the deviations from expected behaviour were attributed to scaling effects that surface out at microscale.

The scaling effect for gas micro-convection is classified into rarefaction and non-rarefaction. The rarefaction scaling effect arises because of failure of continuum assumption. This breakdown is characterized by Kn, defined as ratio of λ and D_h, which is used to explain deviation of fluid from continuum behaviour (rarefaction effect). For $Kn < 0.001$, fluid is assumed to be continnum, which is modelled by Navier–Stokes equation with no slip boundary condition. For $Kn > 10$, fluid is assumed a free molecular flow, which can be modelled with collisionless Boltzmann equation. For $0.001 < Kn < 0.1$, flow regime is slip and first order velocity slip/temperature jump boundary condition is applied to the Navier–Stokes equation. Microdevices work in the range of $0.001 < Kn < 0.1$ and flow is considered with slip boundary condition which lies nearer to continnum. The similarity between rarefied and micro-flow has prompted several authors to investigate along this line, however, this is not a complete similarity [11].

Non-rarefaction effects do not require a modification of Navier–Stokes equation. Therefore, it includes those terms which are prominent at microscale and often neglected due to lack of importance. These terms are axial conduction, viscous dissipation, channel surface condition, compressibility effect and property variation. In micro-convection, temperature gradients along and across the flow are steeper due to small m and low Re and therefore, enable high q''_w because of high surface area. The effects of variation in fluid properties are much stronger, hence, their relative role in micro-convection is significant.

1.1. Review of past work

The fluid flow and heat transfer characteristics in micro-devices with property variation reveal significant differences in

* Corresponding author. Tel.: +91 (0)22 25767122; fax: +91 (0)22 25722602.
E-mail address: spm@aero.iitb.ac.in (S.P. Mahulikar).

0017-9310/$ - see front matter © 2008 Elsevier Ltd. All rights reserved.
doi:10.1016/j.ijheatmasstransfer.2008.08.037

Nomenclature

c	velocity of sound $= \sqrt{\gamma \cdot \Re \cdot T_m}$
$C_p(T)$	temperature dependant specific heat at constant pressure
D	diameter of micro-tube = characteristics dimension = D_h
h	heat transfer coefficient
L	length of micro-tube
m	mass flow rate
p	operating pressure (atmospheric)
r, z	radial and axial cylindrical coordinate
T_m	enthalpy-average temperature of bulk
T_w	temperature of wall
$T(r)$	temperature profile in radial direction
$u(r)$	axial velocity profile in radial direction
$v(r)$	radial velocity profile in radial direction
q''_w	heat flux at wall

Greek symbols

λ	mean free path
γ	specific heat ratio
$\Re$	universal gas constant (=287 J/kg-K)
$\rho(p,T)$	pressure and temperature dependant density
$\mu(T)$	temperature dependant dynamic viscosity
$k(T)$	temperature dependant thermal conductivity
$s_{\rho T}$	temperature-sensitivity of gas density
$s_{\rho p}$	pressure-sensitivity of gas density
$\partial T_m/\partial z$	bulk-mean axial temperature gradient
$(\partial T/\partial r)_w$	radial temperature gradient
$(\partial u/\partial r)_w$	wall-velocity gradient

Dimensionless numbers

Kn	Knudsen number λ/D_h
M	Mach number u_m/c
Nu	Nusselt number hD_h/k_m
Re	Reynolds number $\rho_m u_m D_h/\mu_m$

Subscripts

CP	constant properties
D	based on diameter
in	value at inlet
exit	value at outlet
m	mean value
w	condition at the wall

Abbreviations

MEMS	microelectromechanical system
MST	microsystems technologies
μ-TAS	micrototal analysis systems

quality of convection. It has been observed that property ratio method [12] for correcting Nu fails to predict convection for large q''_w. Further asymptotic theory [13,14] is found to be better applicable for small q''_w and large Re and not suitable for microflows. The role of property variation in micro-convection within continuum regime is investigated during last few years. Mahulikar et al. [15] numerically illustrated the role of gas density variation in determining the induced radial flow and radial convection. A study by Mahulikar and Herwig [16] shows a significant deviation in continuum-based laminar gas micro-convection characteristics due to $\rho(p,T)$, $k(T)$ and $\mu(T)$ variations. They have numerically demonstrated increasing significance of $\mu(T)$ and $k(T)$ variations from macroscale-to-microscale liquid convection [17]. In recent investigation they found higher deviation in convection due to $\mu(T)$ than $k(T)$ variations, although dimensionless temperature sensitivity of viscosity is higher [18]. For circular tube, the dimensionless ratio of radial to axial convection tends to be small towards microscale. Thus, $r_{cv} = \left(\int_0^R v \cdot \frac{\partial T}{\partial r} \cdot r \cdot dr\right) \Big/ \left(\int_0^R u \cdot \frac{\partial T}{\partial z} \cdot r \cdot dr\right) \to O(1)$, hence, radial convection can not be neglected for determining convection characteristics [19].

Experimentally determined Nu for micro-flows was found to be less [2,5] whereas, some researchers [3,4] found its value greater than classical theory. In conventional duct Nu remains constant for laminar forced convection with uniform peripheral wall heat flux [25], however, for gas micro-flow Nu was found to vary significantly with respect to Re [16]. This has been attributed to variation of thermophysical fluid properties, due to large temperature gradients [15,19]. From the literature survey, it is observed that forced laminar gas micro-convection due to $\rho(p,T)$, $C_p(T)$, $\mu(T)$ and $k(T)$ variations with entrance effect is unexplored. The investigations by Mahulikar and Herwig [16–19] in the recent past have been undertaken to understand the physical mechanism of micro-convection. The results presented reveal the significance of property variation and their sensitivities in micro-convection. Further the model extends applicability of computationally inexpensive continuum model to higher Kn situations.

2. Physical model and boundary conditions

Fig. 1 shows schematic of 2D circular tube subjected to different wall heat flux boundary conditions.

Case 1. Entrance length problem: with $q''_w = 7.5\ W/cm^2$ across L_1 and L_2.
Case 2. Graetz problem: with $q''_w = 0$ and $7.5\ W/cm^2$ across L_1 and L_2 respectively.
The following four thermal and flow boundary conditions are incorporated.

(1) *Inlet*: Flat velocity profile: $u(r,0) = u_{in}(r) = u_{m,in} = 20$ m/s and flat temperature profile: $T(r,0) = T(r) = T_{0,in} = 5°C$. The subscript '0' refers to the value of parameter at the axis of micro-tube and mass flow rate is obtained as: $m = \rho(\pi/_4 D^2)u_m$.
(2) *Outlet*: $p_{exit} = 1.013\times10^5$ Pa (atmospheric pressure) and $v_{exit} = 0$ since, $\partial u/\partial z = 0$.
(3) *Wall*: The channel walls are non-porous rigid with $[k(\partial T/\partial r)]_w = q''_w$ and $u_w, v_w = 0$.
(4) *Axis*: Symmetric boundary conditions are applied at the axis of micro-tube, hence, $\partial u/\partial r = \partial T/\partial r = \partial p/\partial r = 0$ and $v = 0$.

Inlet boundary condition reveals the role of property variation mixing with entrance effects. From $z = 0$ and onwards downstream (i.e. throughout entrance region = $L_1 + L_2$) $\rho(p,T)$, $C_p(T)$, $\mu(T)$ and $k(T)$ variations for non-reacting air is modelled.

2.1. Mathematical formulation

The 2D cylindrical co-ordinate (with axisymmetry) continuum-based governing differential equations together with ideal gas equation are numerically solved considering ρ, C_p, μ and k variations.

Continuity:

$$v \cdot (\partial\rho/\partial r) + \rho \cdot (\partial v/\partial r) + (\rho \cdot v/r) + \rho \cdot (\partial u/\partial z) + u \cdot (\partial\rho/\partial z) = 0 \quad (1)$$

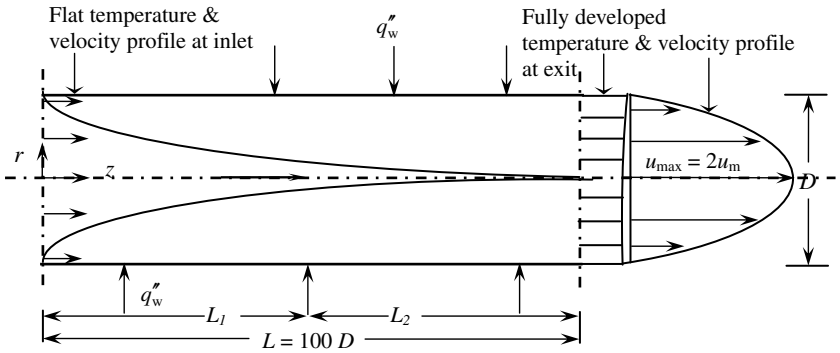

Fig. 1. Schematic of circular tube with wall heat flux boundary condition.

z-momentum:

$$\begin{aligned}\rho\cdot[v\cdot(\partial u/\partial r)+u\cdot(\partial u/\partial z)] = &-(\partial p/\partial z)+\mu\cdot\{(1/3\cdot 1/r)[(\partial v/\partial z)\\ &+3\cdot(\partial u/\partial r)]+[(\partial^2 u/\partial r^2)\\ &+1/3\cdot(\partial^2 v/\partial r\partial z)+4/3\cdot(\partial^2 u/\partial z^2]\}\\ &+\partial\mu/\partial r[(\partial u/\partial r)+(\partial v/\partial z)]\\ &-2/3\cdot\partial\mu/\partial z[(\partial v/\partial r)+(v/r)\\ &-2\cdot(\partial u/\partial z)] \qquad (2)\end{aligned}$$

r-momentum:

$$\begin{aligned}\rho\cdot[v\cdot(\partial v/\partial r)+u\cdot(\partial v/\partial z)] = &-(\partial p/\partial r)+\mu\cdot\{2/3\cdot 1/r\cdot[(\partial v/\partial r)\\ &-(\partial u/\partial z)]+(\partial^2 v/\partial z^2)\\ &+1/3\cdot(\partial^2 u/\partial r\partial z)+4/3\cdot(\partial^2 v/\partial r^2)\}\\ &+(\partial\mu/\partial z)[(\partial u/\partial r)+(\partial v/\partial z)]\\ &-2/3\cdot(\partial\mu/\partial r)[(\partial u/\partial z)+(v/r)\\ &-2\cdot(\partial v/\partial r)] \qquad (3)\end{aligned}$$

energy:

$$\begin{aligned}(\rho\cdot C_p)[u\cdot\partial T/\partial z+v\cdot\partial T/\partial r] = &\,k\cdot(\partial^2 T/\partial r^2)+k/r\cdot(\partial T/\partial r)\\ &+(\partial T/\partial r)\cdot(\partial k/\partial r)+k\cdot(\partial^2 T/\partial z^2)\\ &+(\partial T/\partial z)\cdot(\partial k/\partial z)\\ &+\mu\cdot\{[(\partial v/\partial z)+(\partial u/\partial r)]^2\\ &+(4/3)[(\partial v/\partial r)^2+(v/r)^2\\ &+(\partial u/z)^2]-(4/3)[(\partial v/\partial r)\cdot(v/r)\\ &-(\partial v/\partial r)\cdot(\partial u/\partial z)\\ &-(v/r)\cdot(\partial u/\partial z)]\} \qquad (4)\end{aligned}$$

The u and v are the velocities in z (axial coordinate) and r (radial coordinate) direction. The term containing $\nabla\cdot \mathrm{v} = 1/r\cdot\partial/\partial r(r\cdot v) + \partial u/\partial z$ is incorporated in momentum equation for density variation [27]. Assumptions prescribed in the numerical computation are: flow is laminar, incompressible, steady and non-isothermal. The fluid is considered to be single phase, Newtonian and fluid modelling is within continuum region. Viscous dissipation ($\mu\cdot\{\Phi_v\}$) and compressibility terms in energy equation are neglected. Continuity, Navier–Stokes, energy and ideal gas equations are solved with proper relationship for fluid properties which shows interesting behaviour of energy transfer in a moving fluid.

2.2. Computational domain and numerical solution

To simulate the problem, a mesh is graded in order to capture abrupt change in flow and temperature field, with finer grid in the vicinity of wall. A mesh is 200×50 [=200 (in axial direction) $\times$ 50 (in radial direction)] and grid successive ratio 1.025 axially and 0.95 radially containing 10,000 cells were used. This grid density is selected conservatively based on the grid independence of final result based on Nu_D values. Grid independency was checked for grid aspect ratio ($\Delta z/\Delta r$) = 50, by validating Nu_D results with benchmarked constant properties solution, which yield variation within 0.1%. The global aspect ratio (L/D) is large (=100), where, L is the length of computational domain. The (L/D) value is selected based on (i) fully developed flow at exit, (ii) intricacies of domain, (iii) need to capture the physical mechanism and (iv) computational cost and time.

In the given problem there are four conservation equations [Eqs. (1)–(4)] and five unknown field variables (ρ, u, v, p, T). Hence, for closure incompressible ideal gas equation of state $p = \rho\cdot\Re\cdot T$ is used. The numerical methodology is based on control volume differencing scheme to convert governing equation to algebraic equation. The governing equations with boundary conditions are discretized using *segregated implicit*, second order upwind scheme. For pressure–velocity coupling, simple pressure-differencing scheme is used to secure good convergence. The solution is deemed converged if the plots of residuals for energy, z and r momentum and continuity equations are less than 10^{-12} and independent of number of iterations.

3. Results and discussions

The convective heat transfer in micro-tube is characterized in terms of Nu and interpreted as dimensionless temperature gradient at the surface. It shows the relative significance of heat transfer by the two mechanisms, i.e. axial convection and radial conduction Therefore, Nu for a constant wall heat flux boundary condition reduces to,

$$Nu = q''_w\cdot D/(T_w - T_m)k_m \qquad (5)$$

The following data is fixed for uniformity: R = 375 μm, L = 75 mm and $T_{0,in}$ = 278 K. For some cases results are reproduced with combination of $\rho(p,T)$, $C_p(T)$, $\mu(T)$ and $k(T)$ and their variations for different Re_{in}, L/D and q''_w. For air, $\mu(T)$ variation is given as

$$\mu(T) = 1.462\times 10^{-6}T^{1.5}/(T+112)\ \text{kg/m s, where, } T \text{ is in K} \qquad (6)$$

and $k(T)$ variation is given as [28],

$$k(T) = 2\times 10^{-3}T^{1.5}/(T+112)(\text{where, } T \text{ is in K}) \qquad (7)$$

The $C_p(T)$ is a function of temperature and modelled using sixth-order single piece linear polynomial and scaled between 0 and 1. As shown in Fig. 2 smooth curves are fitted over the range of temperature 200–2000 K within accuracy of 0.12%, which is justified [26].

3.1. Physical effects of variation in gas properties

The $\rho(p,T)$ and $\mu(T)$ variations have indirect effect through velocity (u, v) profiles on Nu whereas, $C_p(T)$ and $k(T)$ variations have direct effect through fluid temperature field.

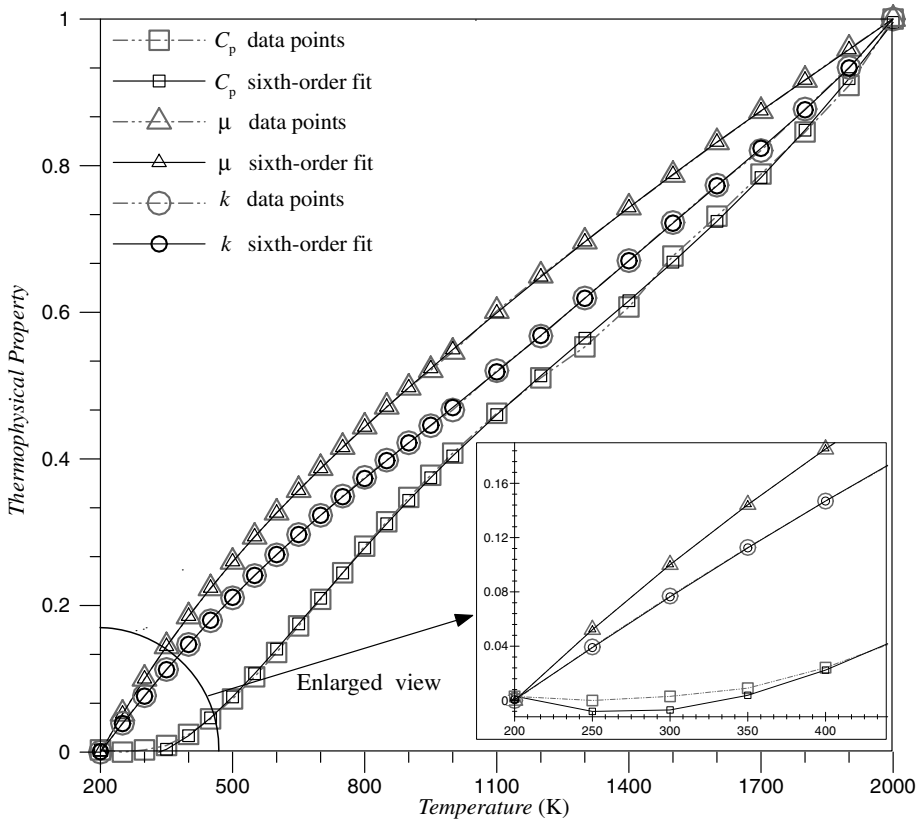

Fig. 2. Corrected sixth-order polynomial fit for C_p, μ and k.

3.1.1. Role of $\rho(p,T)$ variation

Fig. 3(a) illustrates variation in *Nu* along simultaneously developing flow (for $\phi = 750\ \mu m$ tube) with "$q''_w = $ const." boundary condition considering properties variations. The dashed curve shows constant properties solution which is independent of q''_w and two other curve at the bottom shows $\rho(p,T)$ variation with different q''_w.

For $\rho(p,T)$ variation, the radial velocity is zero at $r = 0$ and at $r = R$, and is radially-inward in between axis and wall. The mean velocity is $v_m = -39$ cm/s and -2.5 cm/s at $z/D = 0.5$ and 15, respectively. The $-$ve sign indicates inward radial velocity and its magnitude increases with radius. The cause of inducing radial flow is mean radial velocity and is given by,

$$v_m\left[=\frac{2}{R^2}\cdot\int_0^R v(r)\cdot r\cdot dr\right] \tag{8}$$

For the case of heated air, *Nu* performance with ρ variation can be determined jointly as:

(i) Radially-inward flow is acting in same direction of inward diffusion of temperature due to q''_w. Therefore, radially-inward convection due to v_m actually increases *Nu*.

(ii) But this radially-inward flow causes axial velocity profile to be sharpened (termed as hydrodynamic development of flow) [refer Fig. 4]. The sharpening of $u(r)$ profile results in lowering the axial velocity of moving particles close to wall. For $v(r) < 0$, radially-inward flow promotes convection but sharpened $u(r)$ profile degrades convection. Fig. 4 also shows that sharpening of $u(r)$ decreases $(\partial u/\partial r)_w$ along the flow, thus, $u(r)$ profile is less effective in axial transport of the imposed q''_w, thereby degrading convection.

(iii) The ρ near wall (0.38 kg/m^3) is lower than at axis of tube (1.22 kg/m^3, both values are at $z/D = 15$) which degrades convection. Gas acceleration due to reduce in ρ leads to change velocity profile in magnitude as well as in shape [refer Fig. 4]. Therefore, in the initial part of boundary layer formation net *Nu* reduces abruptly due to sharpening of $u(r)$ profile. It is also observed that *Nu* is minimum at $z/D = 50$ due to following reasons: (a) above-mentioned contradictory mechanism (i) and (ii), (b) induced outward v_m, (c) maximum value of $(T_w - T_m)$ [refer Fig. 5]. The minimum *Nu* (=4.0425) differs from constant properties solution (Nu_{CP}) by 7.4% showing the sensitivity of $\rho(p,T)$ variation.

The result shown in Fig. 3(a) indicates slight increase in *Nu* towards the end of channel. The reason behind this is outward v_m with an induced value of the order of 0.8 cm/s. Fig. 3(a) also shows comparison of $\rho(p,T)$ variation due to $q''_w = 7.5$ and 10 W/cm^2 and it predicts that Nu_{min} is still lower in 10 W/cm^2 case. This has been attributed to: (i) lower density and axial mass flux near the wall and (ii) increase in the value of $(T_w - T_m)$ from 573 to 773 K due to high q''_w.

3.1.2. Role of $\mu(T)$ variation

Fig. 3(a) illustrates variation in *Nu* along flow due to $q''_w = 7.5$ W/cm^2 considering $\mu(T)$ variation. For the case of heated air when entrance effects are considered, the role of $\mu(T)$ variation is to decrease *Nu* compared to the constant properties solution. There are radially-inward velocities which promote *Nu*, but due to sharpening of $u(r,z)$ and $T(r,z)$ profile (resulting from radially-inward flow) *Nu* decreases gradually along the flow.

For the case of heated air, the effect of hydrodynamic development on $u(r,z)$ and $v(r,z)$ profiles is same as that of $\mu(T)$ variation of air. For $q''_w > 0$, the effect of $\mu(T)$ variation is to sharpen $u(r)$ profile by inducing radially-inward $v(r)$ profile. Due to hydrodynamic development of $u(r)$ profile, induced v_m reduces from -6.8 cm/s at $z/D = 5$ to -1.2 cm/s at $z/D = 20$, therefore radially-inward flow is reduced. This provides less sharpening effect of $u(r)$ profile, hence, Nu_{min} is higher for $\mu(T)$ compared to $\rho(p,T)$ variation. The minimum *Nu* (= 4.19) differs from constant properties solution $Nu = \frac{48}{11}$ by 4% showing the sensitivity of $\mu(T)$ variation.

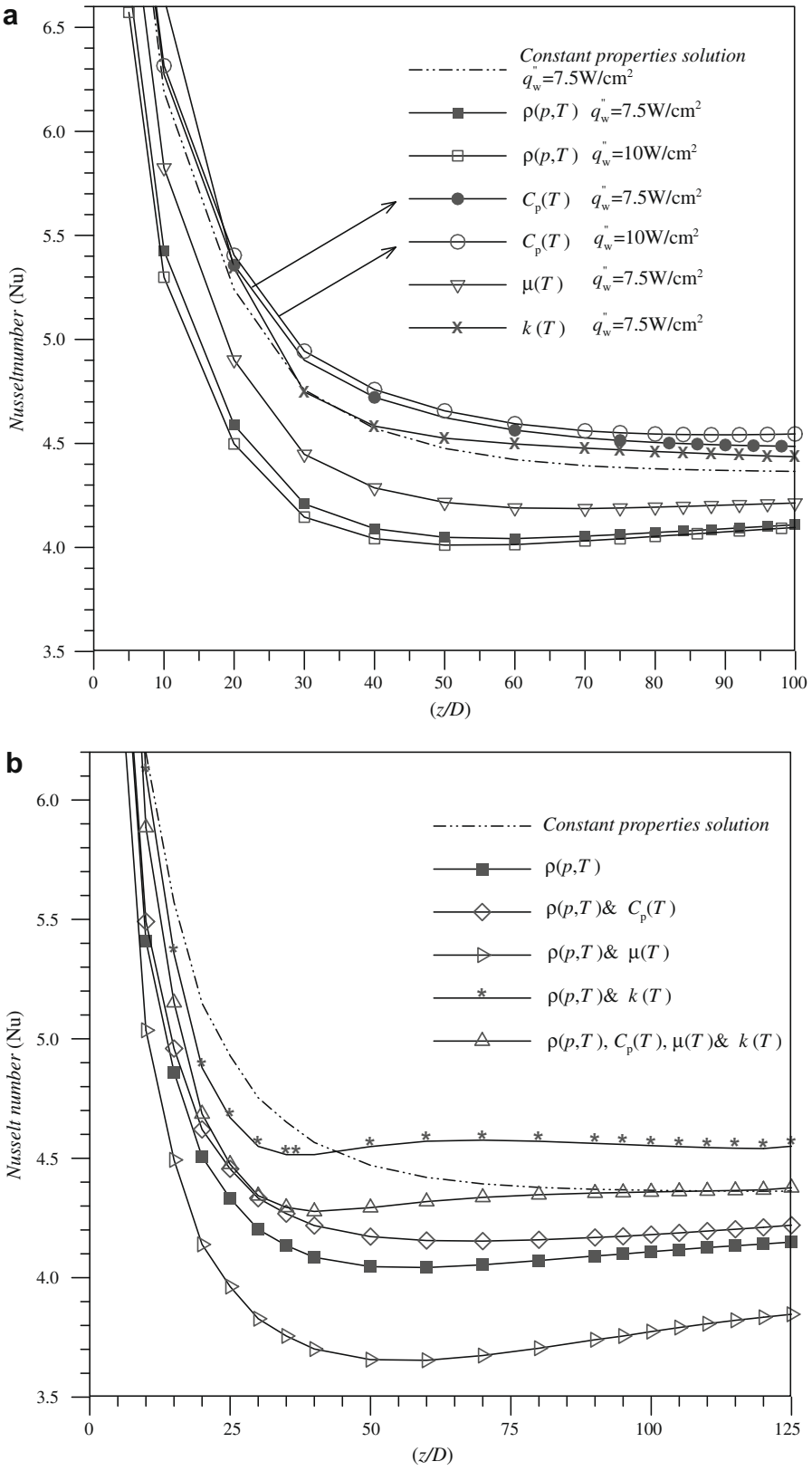

Fig. 3. The *Nu* versus z/D for $u_{m,in}$ = 20 m/s and $q''_w = 7.5$ W/cm^2 with entrance effect (a) due to $\rho(p,T)$, $C_p(T)$, $\mu(T)$ and $k(T)$ variations and (b) due to combination of $\rho(p,T)$, $C_p(T)$, $\mu(T)$ and $k(T)$ variations.

Fig. 3(b) reveals that combine effect of $\rho(p,T)$ and $\mu(T)$ variations is to reduce *Nu* and its rate of decrease aggravates which can be interpreted as follows:

(i) Hydrodynamic-flow development is further enhanced due to induced radially-inward flow with $\rho(p,T)$ and $\mu(T)$ variations.

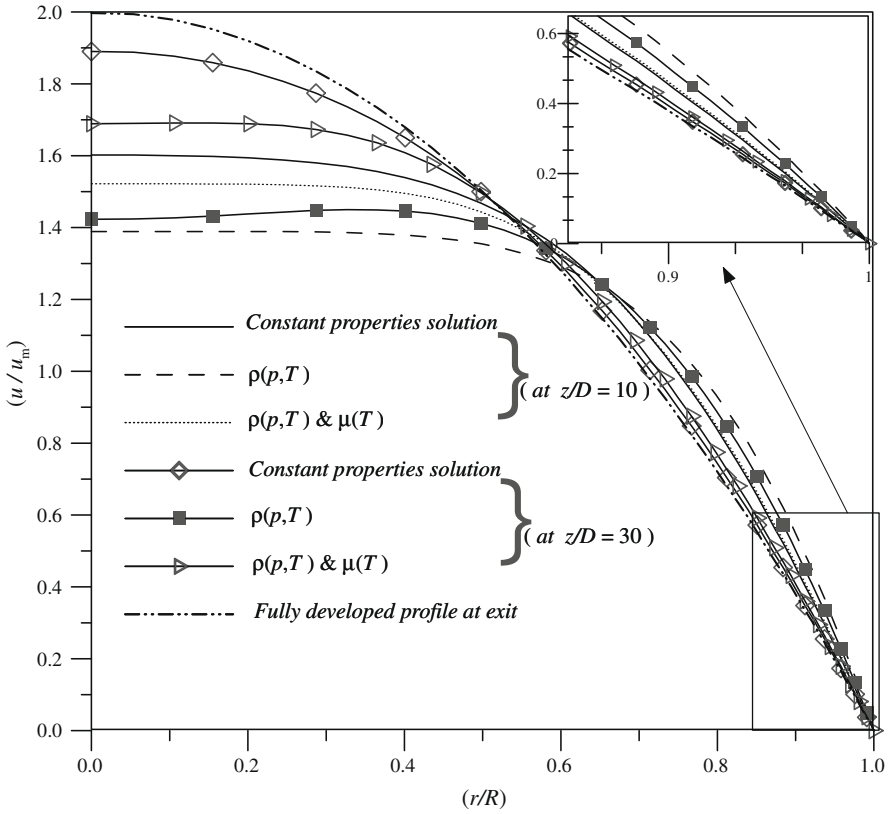

Fig. 4. Variation of axial velocity profile along the flow due to $\rho(p,T)$, $\rho(p,T)$ and $\mu(T)$ variations at several locations for $u_{m,in} = 20$ m/s and $q''_w = 7.5$ W/cm^2.

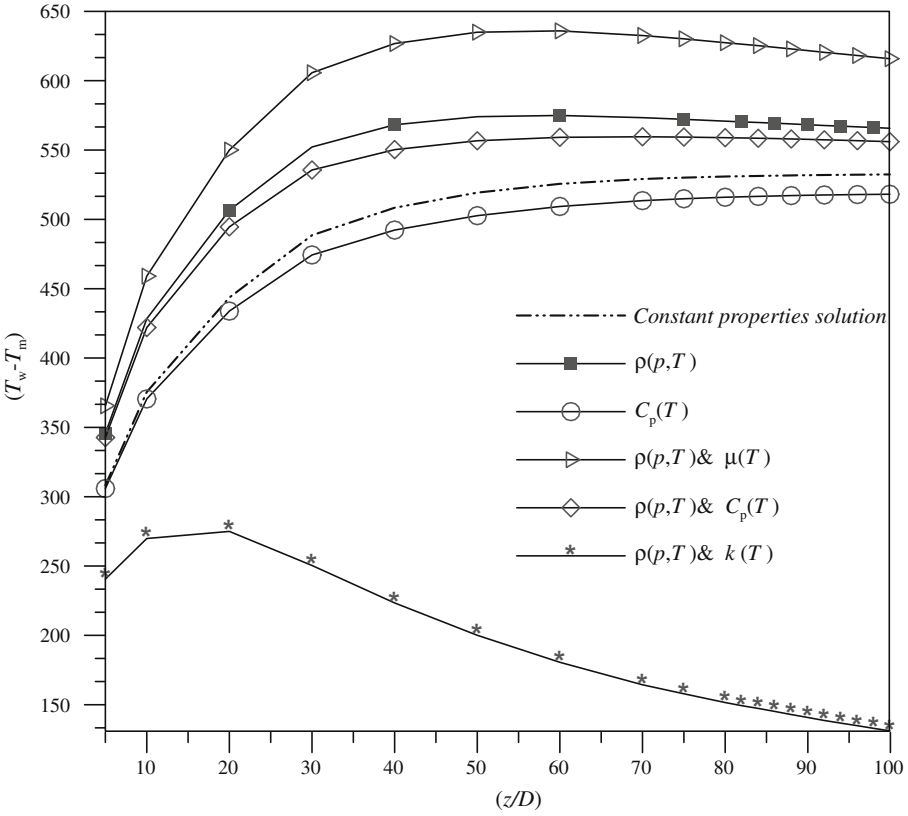

Fig. 5. The $(T_w - T_m)$ versus z/D due to combination of $\rho(p,T)$, $C_p(T)$, $\mu(T)$ and $k(T)$ variations for $u_{m,in} = 20$ m/s and $q''_w = 7.5$ W/cm^2.

(ii) The $\rho(p,T)$ variation renders sharpening of $u(r,z)$ and gas-viscosity increases with temperature that thickens growth of boundary layer. The effect of viscosity penetration results in retardation of fluid particles which causes more resistance to flow and increases boundary layer thickness and eventually decreases h.

(iii) Sharpening of $u(r)$ profile due to $\rho(p,T)$ and $\mu(T)$ variations decreases $(\partial u/\partial r)_w$ compared to $\rho(p,T)$, thereby reducing Nu [refer Fig. 4].

It has been observed that, rate of decrease of Nu is aggravated due to $\rho(p,T)$ and $\mu(T)$ variations. This depends on strength of induced inward radial convection and its dominance is shown in Fig. 3(b). The minimum Nu (=3.65) differs from constant properties solution by 16.3% showing the sensitivity of combine $\rho(p,T)$ and $\mu(T)$ variations. Hydrodynamic flow development due to $\mu(T)$ variation (distorted $u(r,z)$ profile) also exits in conventional channel. But high Re and low q''_w reduces $u(r,z)$ distortion along the flow however, low Re and high q''_w in micro-flow produces $u(r,z)$ distortion by inducing $v(r,z)$ variation. Thus, flow stability is affected by induced radial flow due to property variations [14]. Table 1 shows various flow properties and dimensionless numbers at different locations of geometry (L/D = 100). The use of micro-tube diameter and length ensure that highest Kn in the computational domain is lower by one order of magnitude from, 0.001. The value of Kn is highest at the exit of tube, where ρ is lowest, and exit value of Kn increases with q''_w. The highest M at the exit is less than 0.3; hence, flow can be treated as incompressible. The Re decreases in downstream direction, since, air viscosity increases with temperature. The maximum $T_{w,exit}$ is less than air dissociation temperature and ρ values at exit can differ from 1.225, by about 70%.

3.1.3. Role of $C_p(T)$ variation

Fig. 3(a) illustrates variation in Nu along simultaneously developing flow for "q''_w = const." due to $C_p(T)$ variation. For the case of air being heated, the role of $C_p(T)$ variation is to decrease Nu due to sharpening of $u(r,z)$, $T(r,z)$ profile and it reduces T_w along the flow. It is observed that the effect of $C_p(T)$ variation also results in reduction of T_m. This effect actually decreases Nu as compared to constant properties solution [refer Eq. (5)]. But high $C_p(T)$ near the wall reduces T_w for $q''_w > 0$ and this reduction in T_w compensates for the decrease in T_m. This phenomenon decreases $(T_w - T_m)$, hence, Nu increases along the heated flow [refer Fig. 5 and Eq. (5)]. The T_m is a representative of total energy of flow at a particular location in micro-tube (enthalpy-average temperature of bulk) and is given by,

$$T_m = \frac{\int_0^R \rho \cdot u \cdot C_p \cdot T \cdot r \cdot dr}{\int_0^R \rho \cdot u \cdot C_p \cdot r \cdot dr} \tag{9}$$

From numerical simulation, it is observed that physical effect of $C_p(T)$ variation is more through temperature field than velocity field. Axial temperature gradient $(\partial T_m/\partial z)$ changes with $C_p(T)$ and it increases the variation in property along the flow. For $C_p(T)$ variation rate of decrease of Nu compared to constant properties solution is alleviated, since, it reduces T_w and $(T_w - T_m)$ [refer Fig. 5]. Therefore, Nu_{exit} obtained with $C_p(T)$ variation is higher than constant properties solution, by about 4%. Fig. 3(a) shows increase in Nu_{exit} with increasing q''_w due to $C_p(T)$ variation alone for given Re_{in}. The reason behind this is high q''_w causes more reduction in axial temperature gradient, T_w and $(T_w - T_m)$.

Fig. 3(b) illustrates combine $\rho(p,T)$ and $C_p(T)$ variations due to $q''_w = 7.5$ W/cm^2. The rate of decrease of Nu is higher than constant properties solution, since role of $\rho(p,T)$ is dominant in inducing inward radial flow and sharpening of $u(r,z)$ and $T(r,z)$ profile. But $C_p(T)$ variation is prominent at high temperature region, i.e. towards the end of channel. The $\rho(p,T)$ and $C_p(T)$ variations have decreasing effect on (i) sharpening of temperature profile [refer Fig. 6] (ii) $\partial T_m/\partial z$, (iii) T_w and (iv) $(T_w - T_m)$. The effect of $C_p(T)$ is to reduce radial inward convection, hence, $\rho(p,T)$ and $C_p(T)$ variations contribute to increase in Nu compared to $\rho(T)$ variation alone. The minimum Nu differs from constant properties solution by 4.8% showing the sensitivity of $\rho(p,T)$ and $C_p(T)$ variations. The different values of heat flux due to $\rho(p,T)$ and $C_p(T)$ variations viz. $q''_w = 5, 7.5$

Table 1
Flow properties, wall temperature and dimensionless numbers at different location of geometry with different heat input.

Combination of properties variation with different q''_w	Flow properties at various location of geometry			
	Inlet T_w, T_m ρ_m, C_{pm}, $\mu_m 10^7$, $k_m 10^3$	z/D = 50 T_w, T_m ρ_m, ρ_m, C_{pm}, $\mu_m 10^7$, $k_m 10^3$	Outlet T_w, T_m ρ_m C_{pm}, $\mu_m 10^7$, $k_m 10^3$	$Re_{in,\ exit}$ $M_{in,\ exit} Kn_{in,\ exit} 10^4$
(a) $\rho(p,T)$,$C_p(T)$, $\mu(T)$ and $k(T)$:	366, 278	845, 671	1165, 1042	934, 431
(i) $u_{m,in}$ = 20 m/s, $q''_w = 5$ W/cm^2	1.19, 1004	0.53, 1068	0.34, 1148	0.0575, 0.112
(ii) $u_{m,in}$ = 20 m/s,$q''_w = 7.5$ m/cm^2	183.5, 26	323.4, 50.5	427.6, 70	0.912, 3.842
	407, 278	1075, 857	1534, 1388	888, 351
	1.16, 1005	0.42, 1110	0.25, 1208	0.0575, 0.129
	188.2, 26.8	377.5, 60.5	514, 88.4	0.959, 5.442
(b) $\rho(p,T)$, $C_p(T)$, and $\mu(T)$:	375, 278	1072, 669	1440, 1040	933, 445
(i) $u_{m,in}$ = 20 m/s $q''_w = 5$ W/cm^2	1.19, 1004	0.56, 1068	0.35, 1146	0.0575, 0.116
(ii) $u_{m,in}$ = 20 m/s,$q''_w = 7.5$ W/cm^2	183.7, 24.2	320.9, 24.2	426.3, 24.2	0.913, 3.725
	426, 278	1477, 852	1996, 1384	878, 366
	1.15, 1005	0.45, 1106	0.26, 1209	0.0575, 0.128
	188.8, 24.2	373.6, 24.2	511.3, 24.2	0.971, 5.213
(c) $\rho(p,T)$ and $C_p(T)$:	374, 278	1043, 669	1414, 1040	958, 1059
(i) $u_{m,in}$ = 20 m/s, $q''_w = 5$ W/cm^2	1.19, 1004	0.55, 1068	0.35, 1146	0.0575, 0.116
(ii) $u_{m,in}$ = 20 m/s, $q''_w = 7.5$ W/cm^2	178.9, 24.2	178.9, 24.2	178.9, 24.2	0.889, 1.563
	424, 278	1418, 853	1948, 1385	934, 1047
	1.16, 1005	0.44, 1107	0.26, 1209	0.0575, 0.128
	178.9, 24.2	178.9, 24.2	178.9, 24.2	0.912, 1.823
(d) $\rho(p,T)$:	374, 278	1057, 680	1464, 1089	958, 1046
(i) $u_{m,in}$ = 20 m/s, $q''_w = 5$ W/cm^2	1.19, 1006	0.54, 1006	0.33, 1006	0.0575, 0.114
(ii) $u_{m,in}$ = 20 m/s, $q''_w = 7.5$ W/cm^2	178.9, 24.2	178.9, 24.2	178.9, 24.2	0.889, 1.622
	424, 278	1456, 881	2060, 1495	934, 1043
	1.16, 1006	0.43, 1006	0.24, 1006	0.0575, 0.133
	178.9, 24.2	178.9, 24.2	178.9, 24.2	0.912, 1.901

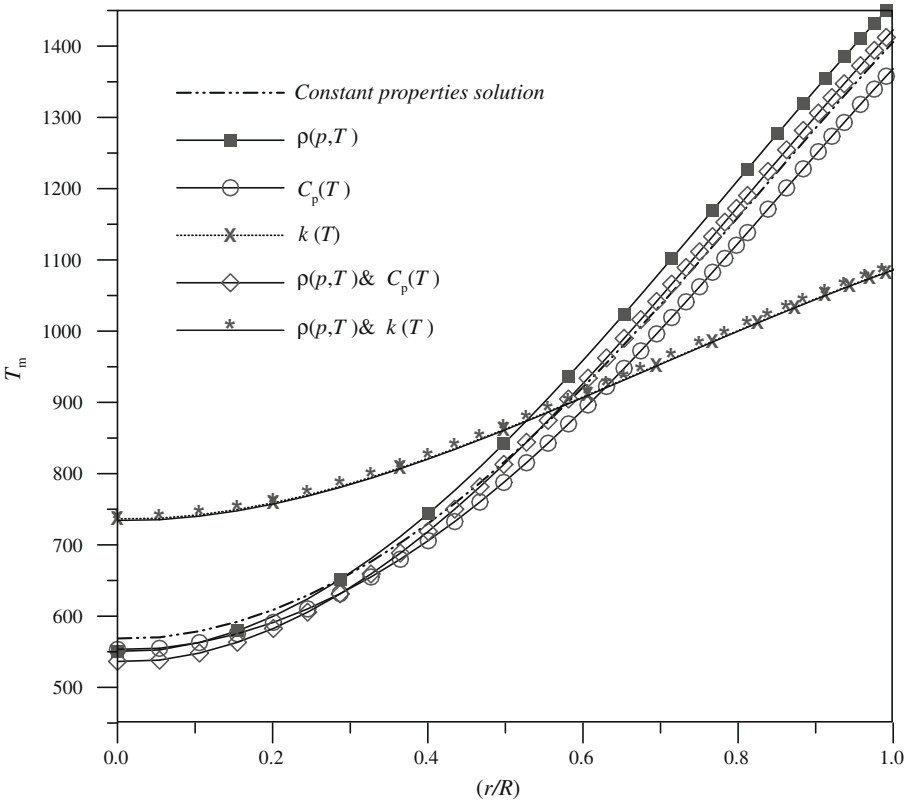

Fig. 6. Variation of radial bulk mean temperature at $z/D = 50$ due to combination of $\rho(P, T)$, $C_p(T)$, $\mu(T)$ and $k(T)$ variations for $u_{m,in} = 20$ m/s and $q''_w = 7.5$ W/cm^2.

and 10 W/cm^2, provides approx. same value of Nu (= 4.22) at exit, which is less than $Nu_{CP.}$

3.1.4. Role of k(T) variation

The role of $k(T)$ [13,20] and additional physical mechanism of $k(T)$ variation is elucidated in the literature [16,18]. Fig. 3(a) illustrates variation in Nu along simultaneously developing flow for "$q''_w = $ const." due to $k(T)$ variation. For the case of heated air, the role of $k(T)$ variation is to decrease Nu due to radially-inward $v(r,z)$ and sharpening of $u(r,z)$, $T(r,z)$ profile. The rate of decrease of Nu is less than constant properties solution which is explained as follows:

The $k(T)$ induces outward radial velocity which counteracts with inward diffusion from wall. Hence, Nu decrease rate is alleviated due to diminishing radially-inward flow.

Heat flow at cross section is given by,

$$q''_w = k_w(\partial T/\partial r)_w. \tag{10}$$

For constant q''_w, increasing k_w along heated flow reduces corresponding temperature gradient near the wall. Higher k-fluid near the wall is more effective in convecting away the imposed thermal boundary condition at the wall, hence, promotes Nu [refer Eq. (10)].

Fig. 6 shows that k variation flattens the temperature profile thus; 'U'-shaped $k(r)$ profile promotes convection relative to Nu_{CP}. The axial gradient is given by [16,18],

$$|\partial T_m/\partial z| = 4(q''_w/D)/\left[(\rho_m \cdot u_m \cdot C_{pm})(\partial k_m/\partial z)\right] \tag{11}$$

The $k(z)$ variation induces axial conduction which significantly affect on micro-convection by increasing $\partial k_m/\partial z$. The higher $\partial k_m/\partial z$ along the heated flow provides large $\partial T_m/\partial z$ which tends to increase Nu [refer Eq. (11)]. Therefore, k variation along and across the flow has the same effect on micro-convection and promotes Nu after minima compared to constant properties solution.

Fig. 3(b) illustrates combine $\rho(p,T)$ and $k(T)$ variations due to $q''_w = 7.5$ W/cm^2. After initial decrease of Nu, role of $k(T)$ is dominant in reducing T_w than inducing inward-radial flow by $\rho(p,T)$. The combine effect of $\rho(p,T)$ and $k(T)$ variations after minima is to induce radially-outward velocities [16]. The magnitude of v_m is 1.5 cm/s at $zD = 30$ and this causes outward flow which flattens $u(r)$ profile. Thus, it promotes convection due to faster moving particle close to the boundary. The $\rho(p,T)$ and $k(T)$ variations also reduces $(T_w - T_m)$ which differs from increase in $(T_w - T_m)$ for constant properties solution, thereby increases Nu [refer Fig. 5 and Eq. (5)]. The $k(T)$ variation and combine $\rho(p,T)$ and $k(T)$ variations decreases the sharpening of temperature profile. This flattens the temperature profile which promotes the convection (refer Fig. 6).

Therefore, Nu is seen to go through minima and increase in Nu after minima is a result of dominance of $k(T)$ variation which is clearly seen in Fig. 3(b). The $Nu = 4.55$ at exit differs from Nu_{CP} by 4.1% which shows sensitivity due to $\rho(p,T)$ and $k(T)$ variations. It is observed that Nu is seen to go through minima in case of (i) $\rho(p,T)$, (ii) $\rho(p,T)$ and $\mu(T)$, (iii) $\rho(p,T)$ and C_p, (iv) $\rho(p,T)$ and $k(T)$ and (v) $\rho(p,T)$, $\mu(T)$, $C_p(T)$ and $k(T)$. The following trend of Nu minima is summarized: $Nu_{min\_(iv)} > Nu_{min\_(v)} > Nu_{min\_(iii)} > Nu_{min\_(i)} > Nu_{min\_(ii)}$.

For $\rho(p,T)$ $C_p(T)$, $\mu(T)$ and $k(T)$ variations, net Nu increases after minima. This is due to contradictory mechanism as follows: (i) the induced inward radial convection due to $\mu(T)$variation, (ii) reduce in T_w and $(T_w - T_m)$ due to $C_p(T)$ variation and (iii) role of $k(T)$ variation is to increase induced radially-outward flow due to $\rho(p,T)$ variation.

The variation in Nu due to $\rho(p,T)$, $\rho(p,T)$ and $C_p(T)$ variations and all properties variations shows an upward trend and seem to approach constant properties solution. It is found that for increase in L/D from 100 to 125, an upward trend remains same and change in Nu_{exit} is within 0.9% for above three cases. Table 2 shows Nu_{exit}

Table 2
The Nu and $|\Delta Nu_{CP}|$ due to $\rho(p,T)$, $C_p(T)$, $\mu(T)$ and $k(T)$ variations with different combination of q''_w, $u_{m,in}$ and $T_{0,in}$.

S. No.	q''_w (W/cm^2)	$u_{m,in}$ (m/s)	$T_{0,in}$ (K)	Nu_{exit}	$\lvert\Delta Nu_{CP}\rvert$ (%)
1	7.5	15	278	4.377	0.32
		20		4.359	0.01
		25		4.347	0.38
2	0.1	20		4.359	0.01
	2.5			4.332	0.64
	5			4.348	0.37
3	7.5	20	274	4.359	0.02
4	2.5	5	278	4.388	0.55
5	2.5	10		4.359	0.11
6	5	10		4.376	0.34

and $|\Delta Nu_{CP}|$ for combination of all properties variations. It has been numerically found that, change in Nu with various combination of q''_w, $u_{m,in}$, and $T_{0,in}$ relative to Nu_{CP} yield within 0.7%. Therefore, Nu for all properties variations is closer to constant properties solution at $z/D = 90$ and onwards. Further, the trend of Nu variation is almost similar towards the end of channel. The geometry beyond $L/D = 125$ has got limitation on Nu behaviour since, maximum fluid temperature should not exceed than its dissociation temperature. Table 3(a) shows Nu_{min} and Nu_{exit} for $u_{m,in} = 20$ m/s and $q''_w = 7.5$ W/cm^2 due to different combination of properties and their variations. The Nu behaviour is verified by conducting numerical experiments with different geometries which yield variation within 4%. It is observed that property variation has insignificant effect on $Nu_{exit}/|\Delta Nu_{CP}|$ except $\rho(p,T)$, $\rho(p,T)$ and $\mu(T)$ variations.

3.2. Graetz problem with variation in properties

Graetz problem incorporating the property variation justifies that effect of density variation is more through its temperature than pressure dependence as $M < 0.3$. It also indicates the coupling between velocity and temperature field and shows the effect of property variation in thermal entrance region once velocity profile is fully developed. Graetz problem involves fully-developed velocity profile and constant mass flow rate and uniform temperature is specified at inlet. Fig. 1 illustrates adiabatic wall ($q''_w = 0$) of length L_1 ($= L/2$) and velocity profile tends to fully-develop at $L/D = 50$. The temperature profile remains flat across L_1, since, there is no heat transfer. Constant wall heat flux (5 W/cm^2) is applied across L_2 to develop temperature profile. The inlet and outlet boundary conditions are similar as described in case 1. For invariant gas properties the flow asymptotes to thermally and hydrodynamically fully-developed at $L/D = 100$ and $Nu_{CP} = \frac{48}{11}$.

3.2.1. Numerical solution and physical mechanism due to variation in properties

For all properties assumed as constant, the velocity field remains same throughout computational domain. This field is already known and independent of temperature substituted in energy equation to obtain partial differential equations (PDEs). Therefore, momentum equation is uncoupled with thermal development of flow. The PDEs can be solved using variable separable method and has an analytical solution. However, when property variation is involved velocity field is coupled with other (temperature, momentum, energy, etc.) fields. This coupling is further enhanced by induced radial flow, hence, it is difficult to obtain an analytical solution. Therefore, it implies that energy equation remains unsolved which is attempted to solve by numerical solution. Jeong and Jeong [21] have studied Graetz problem with slip flow boundary conditions including effect of rarefaction, streamwise conduction and viscous dissipation. Barron et al. [22] modified Graetz problem through slip flow and temperature jump boundary condition and observed that slip flow at boundary augments heat transfer. Several researchers [23,24] work on Graetz problem referred in the literature as extended Graetz problem.

The prime objectives of discussing Graetz problem for variable fluid properties are as follows: (i) to validate importance of gas density sensitivity with respect to pressure and temperature, (ii) to explain coupling between temperature and velocity field. A numerical simulation is done with uniform velocity and temperature to understand the role of property variation coupled with thermal entrance effect.

Fig. 7 illustrates variation in Nu for $\rho(p,T)$, $C_p(T)$, $\mu(T)$ and $k(T)$ variations due to $u_{m,in} = 10$ m/s and $q''_w = 5$ W/cm^2. The gas law has following form, $\rho = \rho_{atm} + \rho_{gauge}/\Re T$ where, p_{atm} is atmospheric value, i.e. operating pressure and local relative (gauge) pressure is zero. Therefore, for incompressible flow, the effect of

Table 3
The Nu_{min} and Nu_{exit} due to different combination of properties and their variations.

S. No.	Nu for combination of properties variations		L/D and D				$\lvert\Delta Nu_{CP}\rvert/Nu_{exit}$	
			$L/D = 100$		$L/D = 125$		$L/D = 125$	
			$D = 750$	$D = 600$	$D = 750$	$D = 600$	$D = 750$	$D = 600$
(a) For $u_{m,in} = 20$ m/s and $q''_w = 7.5$ W/cm^2 with entrance effect								
1	Constant properties	Nu_{exit}	4.365	4.363	4.362	4.363	≅0	≅0
2	$\rho(p,T)$, $C_p(T)$,	Nu_{min}	4.278	4.279	4.277	4.279	0.45	0.44
	$\mu(T)$ and $k(T)$	Nu_{exit}	4.359	4.361	4.376	4.379		
3	$\rho(p,T)$ and $C_p(T)$	Nu_{min}	4.153	4.173	4.153	4.173	1.14	1.03
		Nu_{exit}	4.181	4.207	4.219	4.242		
4	$\rho(p,T)$ and $\mu(T)$	Nu_{min}	3.704	3.734	3.654	3.724	4.23	3.71
		Nu_{exit}	3.776	3.891	3.846	3.957		
5	$\rho(p,T)$ and $k(T)$	Nu_{min}	4.514	4.503	4.515	4.502	0.76	0.7
		Nu_{exit}	4.563	4.529	4.551	4.522		
6	$\rho(p,T)$ only	Nu_{min}	4.043	4.077	4.042	4.079	1.78	1.54
		Nu_{exit}	4.109	4.158	4.149	4.192		

S. No.	Fluid properties	Nu_{min}	$\lvert\Delta Nu_{CP}\rvert$ (%)	Nu_{exit}	$\lvert\Delta Nu_{CP}\rvert/Nu_{exit}$
(b) For $u_{m,in} = 20$ m/s and $q''_w = 7.5$ W/cm^2 with Graetz problem					
1	$\rho(p,T)$	4.076	6.59	4.129	1.59
2	$\mu(T)$	4.204	3.66	4.226	0.87
3	$k(T)$	4.444	1.84	4.444	0.41
4	$\rho(p,T)$ and $\mu(T)$	3.771	13.58	3.851	3.53
5	$C_p(T)$ and $k(T)$	4.478	2.62	4.478	0.59
6	$\rho(p,T)$, $C_p(T)$, $\mu(T)$ and $k(T)$	4.273	2.08	4.351	0.48

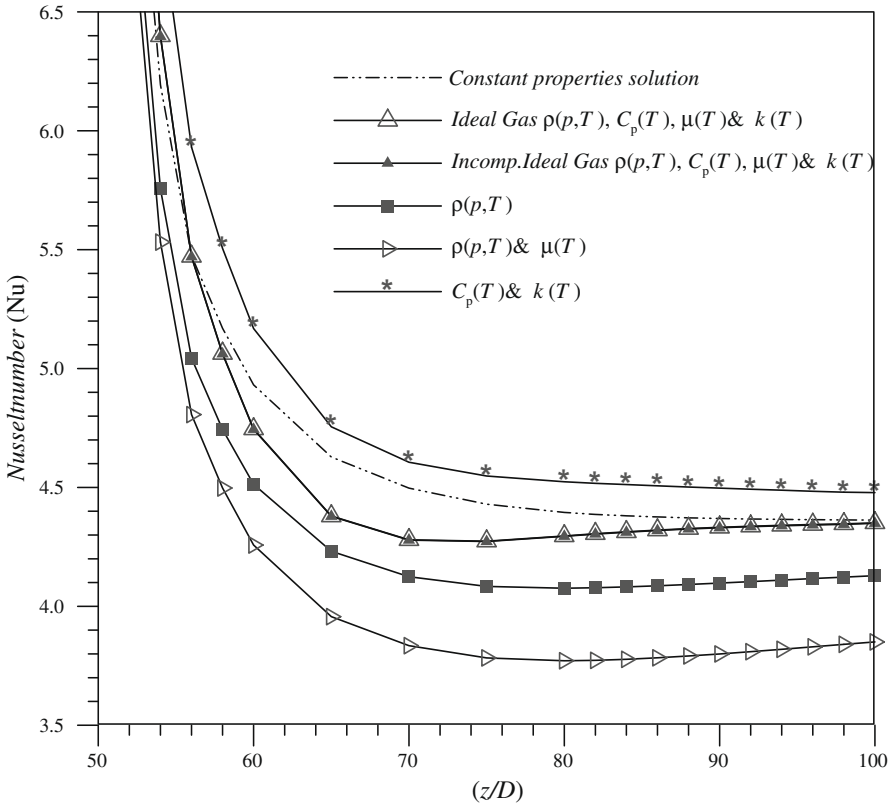

Fig. 7. Variation of *Nu* versus z/D due to combination of $\rho(p,T)$, $C_p(T)$, $\mu(T)$ and $k(T)$ variations for $u_{m,in} = 10$ m/s and $q''_w = 5$ W/cm² with Graetz problem.

density variation is more through its temperature than pressure dependence as $M < 0.3$. The $\rho(p,T)$ variation effects on *Nu* are indicative in micro-convection, due to significant effect of $s_{\rho T}$ resulting from steep temperature gradients. The $s_{\rho p}$ is insignificant, therefore, the deviation of *Nu* between ideal and incompressible ideal gas approximation is negligible. A comparison of *Nu* due to $q''_w = 5$ W/cm² for combination of properties variations is shown in Table 3(b), where minimum *Nu* is differing and

$$|\Delta Nu_{CP}| = [(Nu_{min} - Nu_{CP})/Nu_{CP})] \times 100\%. \quad (12)$$

It is observed that for $\rho(p,T)$, $C_p(T)$, $\mu(T)$ and $k(T)$ variations, *Nu* decreases compared to constant properties solution. The reason for this is explained by various mechanisms due to each property variation as illustrated in Table 4.

This can be jointly explained as follows:

(i) Effect of ρ (p,T) variation is to induce inward radial velocity due to sharpening of $u(r,z)$ and $T(r,z)$ profile, thereby reduces *Nu*. Inward radial flow is in the direction of diffusion of wall boundary condition which is counteracted by outward radial velocity. At $z/D = 80$ and onwards increasing radial velocity flattens $u(r)$ profile, hence, flattening effect increases *Nu*.

(ii) Effect of $C_p(T)$ also becomes relevant due to axial temperature gradients and increases *Nu* towards the end of micro-tube because of reducing $\partial T_m/\partial z$ and $(T_w - T_m)$.

(iii) Effect of $\mu(T)$ variation leads to non-negligible radial convection relative to axial convection and induces inward radial flow by sharpening $u(r)$ profile, thereby reduces *Nu*.

(iv) Effect of $k(T)$ variation is to decrease sharpening of temperature profile and induces non-negligible axial conduction, thereby increases *Nu*. As the gradients are gradually developed, outward radial velocity causes decrease in *Nu* but flattening of temperature profile increases *Nu*.

Table 4
Effect of various thermophysical properties on flow field.

Thermophysical properties	Effect on	
	Velocity field	Temperature field
Density (ρ)	Direct effect. Flattens axial profile (significant)	Direct effect (significant)
Specific heat (C_p)	Indirect effect (insignificant)	Direct effect. Reduces (T_w–T_m) at high temperature (significant)
Viscosity (μ)	Direct effect. Sharpens axial profile (significant)	Indirect effect (insignificant)
Thermal conductivity (k)	Indirect effect. Flattens axial profile (significant)	Direct effect. Flattens temperature profile (significant)

4. Conclusions

(i) Due to sharpening of $u(r,z)$ and $T(r,z)$ profile, resulting from radially-inward flow and contradicting mechanisms involved with each property variation, there occurs a minimum *Nu*. The increase in *Nu* after the minima is a result of dominance of $k(T)$ and $C_p(T)$ variations and reducing *Nu* minima is due to $\mu(T)$ variation.

(ii) The effect of $\rho(p,T)$ and $k(T)$ variations is to induce outward radial velocity which decreases the inward radial flow, hence, rate of decrease of *Nu* is alleviated and *Nu* minima occurs at higher value.

(iii) Gases have lower C_p than liquid which increases axial temperature gradients and the role of property variation along the flow. The role of $C_p(T)$ variation is to reduce $\partial T_m/\partial z$, T_w, and $(T_w - T_m)$, thereby augmenting *Nu*. Reduction in T_w is advantageous for cooling of the wall.

(iv) Graetz problem shows gas density variation with thermal entrance effect at low Mach number due to significance of $s_{\rho T}$ and steep temperature gradients.

Acknowledgments

The authors thank Mr. N.B. Pasalkar, Director Technical Education, Mumbai, India and Government Polytechnic, Thane, India for the support. The authors are grateful to CASDE of their department for the logistics and the A. von Humboldt Foundation, Germany for the rich exposure to research methodology.

References

[1] D.B. Tuckerman, R.F.W. Pease, High-performance heat sinking for VLSI, IEEE Electron. Device. Lett. EDL 2 (1981) 126–129.
[2] X.F. Peng, B.X. Wang, G.P. Peterson, H.B. Ma, Experimental investigation of heat transfer in flat plates with rectangular microchannels, Int. J. Heat Mass Transfer 38 (1995) 127–137.
[3] T.M. Adams, S.I. Abdel-Khalik, S.M. Jeter, Z.H. Qureshi, An experimental investigation of single-phase forced convection in microchannels, Int. J. Heat Mass Transfer 41 (1998) 851–857.
[4] P.Y. Wu, W.A. Little, Measuring of the heat transfer characteristics of gas flow in fine channel heat exchangers for micro miniature refrigerators, Cryogenics 24 (1984) 415–420.
[5] O. Aydin, M. Avci, Heat and fluid flow characteristics of gases in micropipes, Int. J. Heat Mass Transfer 49 (2006) 1723–1730.
[6] F. Sharipov, D. Kalempa, Velocity slip and temperature jump coefficients for gaseous mixtures and viscous slip coefficient, Phys. Fluids 5 (2003) 1800–1806.
[7] G.L. Morini, Single-phase convective heat transfer in microchannels: a review of experimental results, Int. J. Therm. Sci. 43 (2004) 631–651.
[8] M.E. Steinke, S.G. Kandlikar, Review of single-phase heat transfer enhancement techniques for application in microchannels, minichannels and microdevices, Int. J. Heat Technol. 22 (2004) 3–11.
[9] C.B. Sobhan, S.V. Garimella, A comparative analysis of studies on heat transfer and fluid flow in microchannel, Microscale Thermophys. Eng. 5 (2001) 293–311.
[10] S.P. Mahulikar, H. Herwig, O. Hausner, Study of gas micro-convection for synthesis of rarefaction and non-rarefaction effects, J. MEMS 16 (2007) 1543–1556.
[11] M. Gad-el-Hak, Active Flow Control, Cambridge University Press, Cambridge, 2000. pp. 271–307.
[12] S. Kakac, The effect of temperature-dependent fluid properties on convective heat transfer, in: S. Kakac, R.K. Shah, W. Aung (Eds.), Handbook of Single-Phase Convective Heat Transfer, Wiley, New York, 1987, pp. 18.1–18.8.
[13] H. Herwig, The effect of variable properties on momentum and heat transfer in a tube with constant heat flux across the wall, Int. J. Heat Mass Transfer 28 (1985) 423–431.
[14] H. Herwig, P. Schafer, Influence of variable properties on the stability of two-dimensional boundary layers, J. Fluid Mech. 243 (1992) 1–18.
[15] S.P. Mahulikar, H. Herwig, O. Hausner, F. Kock, Laminar gas micro-flow convection characteristics due to steep density gradients, Europhys. Lett. 68 (2004) 811–817.
[16] S.P. Mahulikar, H. Herwig, Physical effects in pure continuum-based laminar micro-convection due to variations of gas properties, J. Phys. D 39 (2006) 4116–4123.
[17] S.P. Mahulikar, H. Herwig, Theoretical investigation of scaling effects from macro-to-microscale convection due to variations in incompressible fluid properties, Appl. Phys. Lett. 86 (2005) 1–3.
[18] S.P. Mahulikar, H. Herwig, Physical effects in laminar micro-convection due to variations in incompressible fluid properties, Phys. Fluids 18 (2006) 1–12.
[19] H. Herwig, S.P. Mahulikar, Variable property effects in single-phase incompressible flows through microchannels, Int. J. Therm. Sci. 45 (2006) 977–981.
[20] K.C. Toh, X.Y. Chen, J.C. Chai, Numerical computation of fluid flow and heat transfer in microchannels, Int. J. Heat Mass Transfer 45 (2002) 5133–5141.
[21] H.E. Jeong, J.T. Jeong, Extended Graetz problem including streamwise conduction viscous dissipation in microchannel, Int. J Heat Mass Transfer 49 (2006) 2151–2157.
[22] R.F. Barron, X.M. Wang, T.A. Ameel, R.O. Warrington, The Graetz problem extended to slip flow, Int. J. Heat Mass Transfer 40 (1997) 1817–1823.
[23] R.S. Myong, D.A. Lockerby, J.M. Reese, The effect of gaseous slip on microscale heat transfer: an extended Graetz problem, Int. J. Heat Mass Transfer 49 (2006) 2502–2513.
[24] G. Tunc, Y. Bayazitoglu, Heat transfer in microtube with viscous dissipation, Int. J. Heat Mass Transfer 44 (2001) 2395–2403.
[25] R. K Shah, A.L. London, Thermal boundary conditions and some solutions for laminar duct flow forced convection, Trans. ASME J. Heat Transfer 40 (1974) 159–165.
[26] J.P. Holman, Heat Transfer, seventh ed., McGraw-Hill, London, 1990.
[27] R.B. Bird, W.E. Stewart, E.N. Lightfoot, Transport Phenomena, second ed., Wiley, New York, 2002 (p. 430, Appendix B).
[28] J.D. Anderson Jr., Hypersonic and High Temperature Gas Dynamics, McGraw-Hill, Singapore, 1989.